PCCP

Accepted Manuscript

ROYAL SOCIETY OF CHEMISTRY

www.rsc.org/pccp

Cite this: DOI: 10.1039/c0xx00000x

www.rsc.org/xxxxxx

ARTICLE TYPE

Direct Synthesis of Mesoporous TiO_2-RuO_2 Composite through Evaporation-Induced Polymeric Micelle Assembly

Bishnu Prasad Bastakoti[a], Rahul R. Salunkhe[a], Jinhua Ye[b], and Yusuke Yamauchi[a,c]*

Received (in XXX, XXX) Xth XXXXXXXXX 20XX, Accepted Xth XXXXXXXXX 20XX

DOI: 10.1039/b000000x

Here we report a direct synthesis of mesoporous TiO_2-RuO_2 composite. Titanium tetraisopropoxide (TTIP) and $RuCl_3$ are used as inorganic precursors for TiO_2 and RuO_2, respectively. Evaporation-induced assembly of spherical micelles made of asymmetric poly(styrene-*b*-2-vinyl pyridine-*b*-ethylene oxide) triblock copolymer enable to fabricate mesoporous TiO_2-RuO_2 composite with uniform pore size of 30 nm.

Various electrochemically active materials, such as transition metal oxides, metal hydroxides, and electronically conducting polymer materials, have been investigated extensively for possible applications in supercapacitors.[1] Supercapacitors have attracted considerable attentions, because they can provide instantaneously a higher power density than batteries and any other conventional dielectric capacitors. Among the metal oxides, ruthenium oxide (RuO_2) shows excellent supercapacitive performance with high capacitance and good reversibility.[2] Structural and compositional controls of RuO_2 electrode materials at a nanometer scale are a critical way to boost the specific capacitance. Low-molecular-weight surfactants and amphiphilic block copolymers have been mostly utilized for the synthesis of mesoporous RuO_2. Recently Sugimoto *et al.* have reported a lyotropic liquid crystal templating for the synthesis of ordered mesoporous Ru and its electrochemical conversion to mesoporous Ru oxide which is applicable to supercapacitor application.[3] A hexagonally ordered mesostructured RuO_2 has been prepared by molecular templates made of sodium 1-dodecanesulfonate through a homogeneous precipitation method.[4] RuO_2-based mesoporous thin films have been also synthesized from Ru-peroxo-based sols using templates made of poly(styrene-*b*-ethylene oxide) diblock copolymers.[5]

Although Ru oxide shows high and stable capacitance than other oxide materials, the rarity and high cost of Ru source always limits its commercial applications. Researchers have been always prompted to identify materials in which Ru could be replaced by other elements or to hybridize Ru with cheaper materials.[6] Several methods (*e.g.*, direct deposition, anodization, impregnation, sputtering, and ball milling) have been demonstrated for hybridization of Ru oxide with other materials.[7] Mesoporous materials with high surface area and large pore volumes are promising materials as supports.[8] Wu *et al.* have reported microwave-assisted hydrothermal process for anchoring of Ru source inside mesopores and synthesized mesoporous SiO_2-RuO_2 composite.[8b] Use of functionalized mesostructured silica appears to give a favourable and simple way to achieve well-controlled and well-dispersed Ru oxide layers inside the mesopores.[8c] However, the above post-treatments require several synthetic steps and sometimes lead to serious pore blocking by the deposited RuO_2. Therefore, there is always a demand for simple and one-pot synthesis method for nanoscale hybridization of RuO_2 with mesoporous matrix.

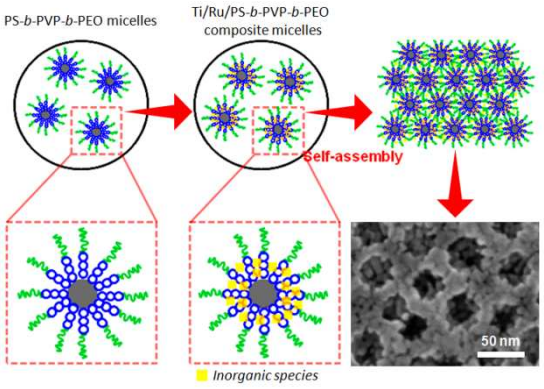

Fig. 1 Synthetic procedure of mesoporous TiO_2-RuO_2 composite through evaporation-induced polymeric micelle assembly.

In this communication, we report a direct synthesis of mesoporous TiO_2-RuO_2 composite. Self-assembly of polymeric micelles and its strong interaction with inorganic source open a new path to synthesize orderly arranged binary mesoporous composite of TiO_2-RuO_2 (**Fig. 1**). Thorough and careful study on the formation of micelles, their interaction with inorganic precursors and the role of stable polymeric micelles as porogens are clearly discussed. Mesoporous TiO_2-RuO_2 composite possesses uniformly sized pores with accessible porosity of guest species from outside.

Synthetic procedure is systematically illustrated in **Fig. 1**. 20 mg of poly (styrene-*b*-2-vinyl pyridine-*b*-ethylene oxide) (PS-*b*-PVP-*b*-PEO) block copolymer was dissolved in 4 mL of THF. The molecular weight of each block is 13000 (PS), 9000 (PVP), and 16500 (PEO), respectively, with polydispersity index 1.15. The polymer was molecularly dissolved in THF, because THF is

a good solvent for each blocks of PS-*b*-PVP-*b*-PEO block copolymer (Tyndall scattering was not confirmed, **Fig. S1a**). After the complete dissolution, 80 µL HCl solution (37 %) was added slowly into the solution. Addition of HCl solution initiates the micellization (Tyndall scattering was clearly confirmed, **Fig. S1b**).[9] $RuCl_3$ solution was added to micelles solution and stirred for 12 h. The final concentration of $RuCl_3$ was 40 mM. Then, TTIP (80 µL) was further added and stirred for 3 h. Here HCl has two roles. Water is poor solvent for PS block so that the polymer undergoes self-assembly to form the spherical micelles. The second one is to assist sol-gel reaction after addition of TTIP. The resulting solution was dried on plastic dish at room temperature. After complete evaporation of solvent, the sample was calcined at 500 ^oC in order to remove the polymeric template.

In the present system, an asymmetric PS-*b*-PVP-*b*-PEO triblock copolymer with chemically distinct functionalities was used as a structure-directing agent for the preparation of mesoporous TiO_2-RuO_2 composite. The presence of micelles was confirmed by dynamic light scattering (DLS) experiment. After addition of HCl solution, the hydrodynamic diameter of polymer micelles was found to be 90 ± 5 nm. When $RuCl_3$ was added into the solution, the Ru^{3+} ions interacted with nitrogen atom of the PVP shells by coordinate bond. It is quite common to form coordinate bonds by transition metal ions to polyvinyl pyridine groups.[10] After further addition of TTIP, the micelle size was reduced to 60 nm. TTIP strongly interacts with PVP blocks.[9] The obtained micelles coordinating with inorganic sources were denoted as 'Ti/Ru/PS-*b*-PVP-*b*-PEO composite micelles'. The decrease in micelle size is attributed to the shrunken conformation of PVP block. **Fig. S2** shows the SEM and TEM images of Ti/Ru/PS-*b*-PVP-*b*-PEO composite micelles. Spherical micelles with average diameter of 55 nm were confirmed. It was clearly observed that the dark shells corresponding to inorganic precursors were covering on the surface of spherical micelles, as indicated by circles in **Fig. S2b**.

The Ti/Ru/PS-*b*-PVP-*b*-PEO composite micellar solution was dried up on plastic dish. As shown in **Fig. 1**, during solvent evaporation, the spherical micelles were closely assembled. After removal of polymer template by calcination, uniformly-sized mesoporous structure with robust and thick wall of TiO_2-RuO_2 was obtained. The surface morphology of mesoporous composite was observed by SEM (**Fig. 2a-b**). The highly magnified SEM image shows that the average pore size is about 30 nm (The mesopore is indicated by circle in **Fig. 2b**). This pore size is larger than those in the previously reported systems using similar block copolymer as template.[11] In the previous report, micelles solution was collected in aqueous medium, but here the presence of THF induced swelling of PS core as it is good solvent for PS block. The PS core sizes of preformed micelles determine pore sizes in final products. The pore sizes and shell thicknesses can be easily tuned by proper selection of block length of PS and PVP, respectively.[9]

In this study, as-prepared sample was calcined at 500 ^oC to remove the polymer template and to induce crystallinity. This temperature is sufficient to remove the polymeric template, as confirmed by TG-DTA. **Fig. S3** shows the TG-DTA curves of Ti/Ru/PS-*b*-PVP-*b*-PEO composite micelles. The large weight loss at 300-400 ^oC indicates the removal of polymer. In general, when low-molecular-weight surfactants or block copolymers are used, the original mesostructures are distorted and/or destroyed with increase of calcination temperatures.[12] In the present study, however, the mesoporosity was completely preserved even when the calcination temperature was higher than the crystallization temperature of TiO_2 and RuO_2 phases. In comparison to other systems using Pluronic-type block copolymers (*e.g.*, P123, F127)[12], PS-*b*-PVP-*b*-PEO block copolymer used in this study is thermally stable (**Fig. S3**) and contain the remnant of polymer during calcination which are beneficial to get the ordered structures of mesoporous materials. Such *in-situ* formed polymer derivatives preserve the mesoporosity even at high temperature.

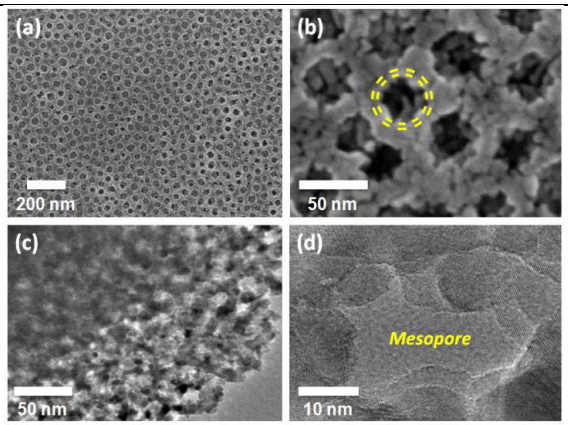

Fig. 2 SEM and TEM images of mesoporous TiO_2-RuO_2 composite. One mesopore are indicated by a yellow-colored circle.

Fig 2c-d shows the TEM image of mesoporous TiO_2-RuO_2 composite. The HR-TEM images (**Fig. 2d** and **Fig. S4**) of mesoporous TiO_2-RuO_2 composite show polycrystalline structure with different crystallites and domain sizes. From elemental mapping, both TiO_2 and RuO_2 phases were uniformly distributed over the entire area. Any pores blocking, which has been often seen in post-treatment process for preparation of mesoporous composite, was not confirmed at all. One-pot and simultaneous synthetic approach is very useful for preparation of mesoporous composite materials. N_2 adsorption desorption isotherms of mesoporous TiO_2-RuO_2 composite is shown in **Fig. S5**. Type IV isotherm, which is representative of mesoporous materials was confirmed. The surface area was found to be 45 $m^2 \cdot g^{-1}$. The pore size distribution curve is also shown in the inset of **Fig. S5**. The average pore size was almost similar as the result in electron microscope images (**Fig. 2b**).

From wide-angle XRD profile of mesoporous TiO_2-RuO_2 composite (**Fig. 3**), several peaks were assigned and matched with tetragonal RuO_2 crystal (JCPDS 00-043-1027). The other peaks were assigned with TiO_2 in anatase form (JCPDS 00-021-1272). For comparison, mesoporous TiO_2 prepared from the same synthetic way are also shown, in which all the peaks were

assigned with anatase phase. The crystalline size of TiO_2 and RuO_2 in the mesoporous composite were calculated by using Sherrer equation and found around 18 nm and 10 nm for TiO_2 and RuO_2, respectively, meaning that both Ti and Ru atoms were not atomically mixed, but totally separated to form nanocomposite consisting of small-sized TiO_2 and RuO_2 crystals. X-ray photoelectron spectroscopy (XPS) study was carried out in order to investigate the chemical compositions of mesoporous TiO_2-RuO_2 composite and oxidation states of Ti and Ru atoms (**Fig. S6**). Titanium, oxygen, and ruthenium related peaks were detected. The high-resolution XPS spectra in **Fig. S6a** show that there are two peaks at 460 eV and 465.5 eV, which are assigned to Ti $2p_{3/2}$ and Ti $2p_{1/2}$, respectively. The peak positions and the separation of two peaks by 5.5 eV confirm Ti^{4+} oxidation state.[13a] Similarly, Ru $3d_{5/2}$ peak at 281.76 eV and Ru $3d_{3/2}$ peak at 285.93 eV indicate the existence of Ru^{4+} cations as expected for RuO_2 (**Fig. S6b**).[13b] The XPS results reveal that the obtained mesoporous composite contains TiO_2 and RuO_2 phase. The compositional ratio of (atomic%) TiO_2:RuO_2 was measured to be 35:1.

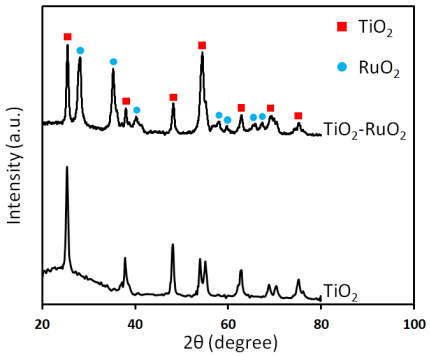

Fig. 3 Wide-angle XRD profiles of mesoporous TiO_2-RuO_2 composite and mesoporous TiO_2.

The electrochemical performance of mesoporous TiO_2-RuO_2 composite was studied using cyclic voltammetry (CV) studies. Mesoporous TiO_2-RuO_2 composite coated on graphite substrate is used as working electrode, whereas Pt wire and Ag/AgCl electrode are used as counter and reference electrode, respectively. **Fig. S7a** shows the typical cyclic voltammograms at different scanning rate in 0.5 M H_2SO_4. The supercapacitor electrode exhibited very good stable operation with redox peak positions at 0.35 and 0.5 V potentials. The specific capacitance (C_{sp}) is calculated by using equation,

$$C_{sp} = \frac{1}{ms(V_f - V_i)} \int_{V_i}^{V_f} I(V)dv$$

where C_{sp} is the specific capacitance ($F \cdot g^{-1}$), m is the mass of the active electrode material (g), s is the potential scan rate ($mV \cdot s^{-1}$), V_f and V_i are the integration limits of the voltammetric curve (V), and $I(V)$ denotes the response current density ($A \cdot cm^{-2}$).

In the case of mesoporous TiO_2, the capacitive current responses were quite small (**Fig. S8**), suggesting that the pristine TiO_2 shows irreversible reducible characteristics. The non-ideal capacitive property is ascribed to the poor electronic conductivity of TiO_2. In contrast, mesoporous TiO_2-RuO_2 composite showed good supercapacitor performance. Mesoporous TiO_2-RuO_2 composite exhibited capacitance value of 110, 72, 59, 50, 45 $F \cdot g^{-1}$ at the scan rate of 20, 40, 60, 80 and 100 $mV \cdot s^{-1}$ respectively (**Fig. S7b**). Higher scan rates result in shorter redox times, leading to the incomplete redox transitions of the "inner" active sites. The observed capacitance value of mesoporous TiO_2-RuO_2 composite is much higher than those of mesoporous TiO_2 (0.34 $F \cdot g^{-1}$ at 20 $mV \cdot s^{-1}$, **Fig. S8**) and relatively higher than those of previously reported TiO_2-based composites (*e.g.*, TiO_2/carbon nanotube composite[14]). Our data demonstrate importance of synergy effect of our composite as well as total utilization of porous space inside material by addition of electroconductive RuO_2 phase. Further optimization about effect of compositional ratios of RuO_2 and TiO_2 on capacitor performance is under consideration in our further studies.

In summary, we demonstrated very simple, one-step synthetic method for mesoporous binary oxides of TiO_2 and RuO_2 using polymeric micelle assembly approach for the first time. The PS cores in the spherical micelles form the mesopores after removing template and the PVP shells are reaction sites for inorganic source. The hydrophilic corona stabilizes the dispersed micelles in solution and helps for their orderly organization during solvent evaporation. Our facile one-pot approach can provide an easy access to many different metal oxides for various applications.

Notes and references

a *World Premier International (WPI) Research Center for Materials Nanoarchitectonics, National Institute for Materials Science (NIMS), 1-1 Namiki, Tsukuba, Ibaraki 305-0044, Japan. E-mail: YAMAUCHI.Yusuke@nims.go.jp*

b *Environmental Remediation Materials Unit, National Institute for Materials Science (NIMS), 1-1 Namiki, Tsukuba, Ibaraki 305-0044, Japan.*

c *Precursory Research for Embryonic Science and Technology (PRESTO), Japan Science and Technology Agency (JST), 2-1 Hirosawa, Wako, Saitama 351-0198, Japan.*

† *Electronic Supplementary Information (ESI) available: Experimental details and characterization data of Ti/Ru/PS-b-PVP-b-PEO composite micelles and mesoporous TiO_2-RuO_2 composite.*

References

[1] (a) M. Winter and R. J. Brodd, *Chem. Rev.*, 2004, **104**, 4245. (b) G. Wang, L. Zhang and J. Zhang, *Chem. Soc. Rev.*, 2012, **41**, 797. (c) W. Wei, X. Cui, W. Chen and D. G. Ivey, *Chem. Soc. Rev.*, 2011, **40**, 1697. (d) B. P. Bastakoti, H. S. Huang, L. C. Chen, K. C. W. Wu and Y. Yamauchi, *Chem. Commun*., 2012, **48**, 9150. (e) B. P. Bastakoti, H. Oveisi, C. C. Hu, K. C. W. Wu, N. Suzuki, K. Takai, Y. Kamachi and Y. Yamauchi, *Eur. J. Inorg. Chem.*, **2013**, 1109. (f) B. P. Bastakoti, Y. Kamachi, H. S. Huang, L. C. Chen, K. C. W. Wu and Y. Yamauchi, *Eur. J. Inorg. Chem.*, 2013, **2013**, 39.

[2] (a) W. Sugimoto, H. Iwata, Y. Yasunaga, Y. Murakami and Y. Takasu, *Angew. Chem. Int. Ed.* 2003, **42**, 4092. (b) V. Ozolins, F. Zhou and M. Asta, *Acc. Chem. Res*., 2013, **46**, 1084. (d) C. Yuan, L. Chen, B. Gao, L. Su and X. Zhang, *J. Mater. Chem.*, 2009, **19**, 246.

[3] (a) W. Sugimoto, S. Makino, R. Mukai, Y. Tatsumi, K. Fukuda, Y. Takasu and Y. Yamauchi, *J. Power Sources*, 2012, **204**, 244. (b) S. Makino, Y. Yamauchi and W. Sugimoto, *J. Power Sources*, 2013, **227**, 153.

[4] Y. Inoue, M. Uota, M. Uchigasaki, S. Nishi, T. Torikai, T. Watari and M. Yada, *Chem. Mater.*, 2008, **20**, 5652.

[5] C. Sassoye, C. Laberty, H. L. Khanh, S. Cassaignon, C. Boissiere, M. Antonietti and C. Sanchez, *Adv. Funct. Mater.,* 2009, **19**, 1922.

[6] (a) P. Soudan, J. Gaudet, D. Guay, D. Belanger and R. Schulz, *Chem. Mater*. 2002, **14**, 1210. (b) M. Wu, *Appl. Phys. Lett*. 2005, **87**, 153102. (c) C. Yuan, L. Chen, B. Gao, L. Su and X. Zhang, *J. Mater. Chem.*, 2009, **19**, 246. (d) J. W. Ko, W. H. Ryu, Il-D. Kim and C. B. Park, *Chem. Commun*., 2013, **49**, 9725. (e) I. L. Chen, T. Y. Chen, C. C. Hu and C. H. Lee, *J. Mater. Chem. A,* 2013, **1**, 2039.

[7] (a) J. Xu, Q. Wang, X. Wang, Q. Xiang, B. Liang, D. Chen and G. Shen, *ACS Nano.*, 2013, **7**, 5453. (b) J. H. Kim, K. Zhu, Y. Yan, C. L. Perkins and A. J. Frank, *Nano Lett.*, 2010, **10**, 4099. (c) Z. R. Cormier, H.A. Andreas and P. Zhang, *J. Phys. Chem. C*, 2011, **115**, 19117. (d) J. Zang, S. J. Bao, C. M. Li, H. Bian, X. Cui, Q. Bao, C. Q. Sun, J. Guo and K. Lian, *J. Phys. Chem. C*, 2008, **112**, 14843. (e) P. Soudan, J. Gaudet, D. Guay, D. Belanger and R. Schulz, *Chem. Mater.*, 2002, **14**, 1210.

[8] (a) K. Ariga, A. Vinu, Y. Yamauchi, Q. Ji and J. P. Hill, *Bull. Chem. Soc. Jpn.*, 2012, **85**, 1. (b) H. S. Huang, K. H. Chang, N. Suzuki, Y. Yamauchi, C. C. Hu and K. C. W. Wu, *Small,* 2013, **9**, 2520. (c) S. Jansat, K. Pelzer, J. G.-Antón, R. Raucoules, K. Philippot, A. Maisonnat, B. Chaudret, Y.Guari, A. Mehdi, C. Reyé and R. J. P. Corriu, *Adv. Funct. Mater.,* 2007, **17**, 3339. (d) K. Ariga, Y. Yamauchi, G. Rydzek, Q. Ji, Y. Yonamine, K. C. W. Wu and J. P. Hill, *Chem. Lett*., 2014, **1**, 36. (e) H. Y. Lian, Y. H. Liang, Y. Yamauchi, and K. C. W. Wu, *J. Phys. Chem. C*, 2011, **115**, 6581.

[9] B. P. Bastakoti, N. L. Torad and Y. Yamauchi, *ACS Appl. Mater. Interface*, 2014, **6**, 854. (b) B. P. Bastakoti, S. Ishihara, S. Y. Leo, K. Ariga, K. C. W. Wu and Y. Yamauchi, *Langmuir*, 2014, **30**, 651.

[10] (a) Z. Sun, F. Bai, H. Wu, D. M. Boye and H. Fan, *Chem. Mater.*, 2012, **24**, 3415. (b) D. H. Lee, H. Y. Kim, J. K. Kim, J. Huh and D. Y. Ryu, *Macromolecules*, 2006, **39**, 2027. (c) B. H. Sohn, J. M. Choi, S. Yoo, S. H. Yun, W. C. Zin, J. C. Jung, M. Kanehara, T. Hirata and T. Teranishi, *J. Am. Chem. Soc.*, 2003, **125**, 6368. (d) J. J. Chiu, B. J. Kim, E. J. Kramer and David J. Pine, *J. Am. Chem. Soc*., 2005, **127**, 5036.

[11] B. P. Bastakoti, M. Imura, Y. Nemoto and Y. Yamauchi, *Chem. Commun*., 2012, **48**, 12091.

[12] M. B. Zakaria, N. Suzuki, N. L. Torad, M. Matsuura, K. Maekawa, H. Tanabe andY. Yamauchi, *Euro. J. Inorg. Chem.* 2013, **2013**, 2330.

[13] (a) M. T. Uddin, Y. Nicolas, C. Olivier, T. Toupance, M. M. Mu□ller, H. J. Kleebe, K. Rachut, J. Ziegler, A. Klein and W. Jaegermann, *J. Phys. Chem. C,* 2013, **117**, 22098. (b) R. Schafranek, J. Schaffner and A. Klein, *J. Eur. Ceram. Soc*., 2010, **30**, 187.

[14] X. Sun, M. Xie, J. J. Travis, G. Wang, H. Sun, J. Lian, S. M. George, *J. Phys. Chem. C*, 2013, **117**, 22497.

A table of contents

Direct Synthesis of Mesoporous TiO_2-RuO_2 Composite through Evaporation-Induced Polymeric Micelle Assembly

Bishnu Prasad Bastakoti, Rahul R. Salunkhe, Jinhua Ye, and Yusuke Yamauchi*

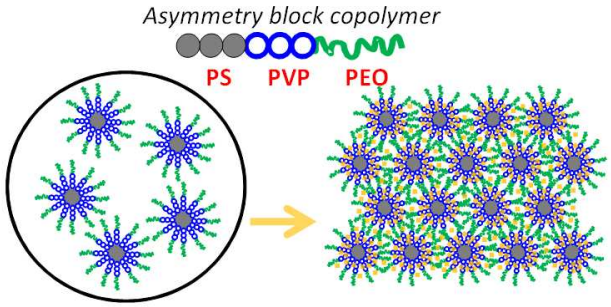

Evaporation-induced assembly of spherical micelles made of asymmetric triblock copolymer enable to fabricate mesoporous TiO_2-RuO_2 composite with uniform pore size.